HOLLOWNESS IN *pp* SCATTERING[*] [**]

Wojciech Broniowski

The H. Niewodniczański Institute of Nuclear Physics, Polish Academy of Sciences
Kraków, Poland
and
Institute of Physics, Jan Kochanowski University, Kielce, Poland
Wojciech.Broniowski@ifj.edu.pl

Enrique Ruiz Arriola

Departamento de Física Atómica, Molecular y Nuclear and
Instituto Carlos I de Fisica Teórica y Computacional, Universidad de Granada,
Granada, Spain
earriola@ugr.es

(Received April 10, 2017)

It is argued that the hollowness effect (depletion in the absorptive part of the scattering cross section at small values of the impact parameter) in the proton–proton scattering at the LHC energies finds its origin in the quantum nature of the process, resulting in large values of the real part of the eikonal phase. The effect cannot be reconciled with an incoherent superposition of the absorption from the proton constituents, thus suggests the change of this basic paradigm of high-energy scattering.

DOI:10.5506/APhysPolB.48.927

In this talk, we discuss the significance of the recent *pp* scattering results from the Large Hadron Collider for our understanding of the underlying physical processes in highest-energy collisions. In particular, we argue that the *hollowness* in the inelastic cross section treated as a function of the impact parameter b, *i.e.*, its depletion at low b, must necessarily originate from quantum coherence, precluding a probabilistic folding interpretation. More details of our analysis can be found in [1, 2], where we also analyze the effect in 3 dimensions via the optical potential interpretation.

[*] Presented by W. Broniowski at the Cracow Epiphany Conference "Particle Theory Meets the First Data from LHC Run 2", Kraków, Poland, January 9–12, 2017.

[**] Supported by the Polish National Science Center (NCN) grant 2015/19/B/ST2/00937, by the Spanish Mineco Grant FIS2014-59386-P, and by Junta de Andalucía grant FQM225-05.

The TOTEM [3] and ATLAS (ALFA) [4] collaborations have measured the differential elastic cross section for the pp collisions at $\sqrt{s} = 7$ TeV, later repeated for $\sqrt{s} = 8$ TeV [5, 6]. When the data are used to obtain the inelastic cross section in the impact-parameter representation, a striking feature appears: there is more inelasticity when the two protons are separated by about half a fermi in the traverse direction than for the head-on collisions. We term this phenomenon *hollowness*. This unusual feature has been brought up and interpreted by other authors [7–15]. A model realization of the effect was implemented via hot-spots in [16].

We use the parametrization of the pp scattering data [17] based on the Barger–Phillips model (modified BP2) [18] of the form of

$$\mathcal{A}(s,t) \equiv \frac{f(s,t)}{p} = \sum_n c_n(s) F_n(t) s^{\alpha_n(t)} = \frac{i\sqrt{A}e^{\frac{Bt}{2}}}{\left(1-\frac{t}{t_0}\right)^4} + i\sqrt{C}e^{\frac{Dt}{2}+i\phi}\,, \quad (1)$$

where $f(s,t)$ is the quantum mechanical scattering amplitude. The modified BP2 model deals with the t dependence and the s-dependent parameters are fitted separately to the differential elastic pp cross sections at $\sqrt{s} = 23.4$, 30.5, 44.6, 52.8, 62.0, and 7000 GeV. A typical quality of the fit, from the ISR [19] at $\sqrt{s} = 23.4$ GeV to the LHC at $\sqrt{s} = 7$ TeV, can be appreciated from Fig. 1 (a). These fits are not sensitive to the *phase* of the scattering amplitude.

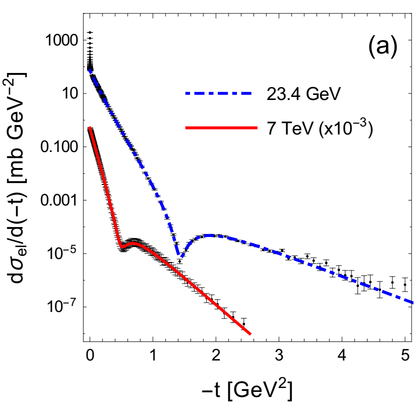

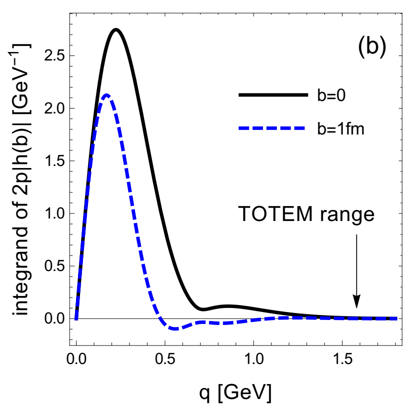

Fig. 1. (a) The data for the ISR energy of $\sqrt{s} = 23.4$ GeV [19] and the LHC energy of $\sqrt{s} = 7$ TeV [3] with overlaid fits according to Eq. (1). (b) Plot of the integrand of Eq. (6) showing that the range of the experimental data in q is sufficient to carry out the Fourier–Bessel transform for the values of b of interest.

The $\rho(s)$ parameter is defined as the ratio of the real-to-imaginary parts of the amplitude at $t = 0$

$$\rho(s) = \frac{\mathrm{Re}\,\mathcal{A}(s,0)}{\mathrm{Im}\,\mathcal{A}(s,0)}\,. \tag{2}$$

This parameter has been recently determined for the LHC energy of $\sqrt{s} = 8$ TeV in [20]. To agree with this experimental constraint, we replace the parametrization of the scattering amplitude of Eq. (1) with

$$\mathcal{A}(s,t) \to \frac{i + \rho(s)}{\sqrt{1+\rho(s)^2}}\,|\mathcal{A}(s,t)|\,. \tag{3}$$

This procedure assumes a t-independent ratio of the real-to-imaginary parts of the scattering amplitude for all t-values, which is the simplest choice. More general prescriptions have been analyzed in detail in Ref. [20]. Our results presented below are similar if we take, *e.g.*, the Bailly *et al.* [21] parametrization $\rho(s,t) = \rho_0(s)/(1 - t/t_0(s))$, where $t_0(s)$ is the position of the diffractive minimum. However, admittedly, there is some dependence on the choice of the model of $\rho(s,t)$. Moreover, the problem is linked to the separation of the Coulomb and strong amplitudes. The issue is crucial for the proper extraction of the physical results and the ambiguity has a long history since the early diagrammatic work of West and Yennie [22], which is consistent with the eikonal approximation [23, 24] but becomes sensitive to internal structure from electromagnetic information such as form factors (see, *e.g.*, [25] and references therein).

Our prescription (3) maintains by construction the quality of the fits shown in Fig. 1, but also the experimental values for $\rho(s)$ are reproduced, which would not be the case if Eq. (1) were used. Basic physical quantities stemming from our method are listed in Table I, with a good agreement with the data supporting the used parametrization.

We now recall the relevant formulas from scattering theory: The *pp* elastic differential cross section is given by

$$\frac{\mathrm{d}\sigma_{\mathrm{el}}}{\mathrm{d}t} = \frac{\pi}{p^2}\frac{\mathrm{d}\sigma_{\mathrm{el}}}{\mathrm{d}\Omega} = \frac{\pi}{p^2}|f(s,t)|^2 = \pi|\mathcal{A}(s,t)|^2\,, \tag{4}$$

with $p = \sqrt{s/4 - M^2}$ the CM momentum and the partial wave expansion of the scattering amplitude (we neglect spin effects) equal to

$$f(s,t) = \sum_{l=0}^{\infty}(2l+1)f_l(p)P_l(\cos\theta)\,. \tag{5}$$

TABLE I

Basic scattering observables for several collision energies obtained from Eq. (3), compared to experimental values (lower rows). B is the slope parameter of the differential elastic cross section.

$\sqrt{s}$ [GeV]	$\sigma_{\rm el}$ [mb]	$\sigma_{\rm in}$ [mb]	$\sigma_{\rm T}$ [mb]	B $\left[\mathrm{GeV}^{-2}\right]$	ρ
23.4	6.6	31.2	37.7	11.6	0.00
[19]	6.7(1)	32.2(1)	38.9(2)	11.8(3)	0.02(5)
200	10.0	40.9	50.9	14.4	0.13
[26, 27]			54(4)	16.3(25)	
7000	25.3	73.5	98.8	20.5	0.140
[3]	25.4(11)	73.2(13)	98.6(22)	19.9(3)	0.145(100)

The total cross section is given by the optical theorem, $\sigma_{\rm T} = 4\pi \,{\rm Im}\, f(s,0)/p$, and Coulomb effects are negligible at $|t| > 8\pi\alpha/\sigma_{\rm T}$, where $\alpha \simeq 1/137$ is the QED fine structure constant and $\sigma_{\rm T}$ is the total strong scattering cross section. For $pa \gg 1$, with a denoting the interaction range, one can use the eikonal approximation with $bp = l + 1/2 + \mathcal{O}(s^{-1})$, where b is the impact parameter. The b representation of the scattering amplitude can be straightforwardly obtained from a Fourier–Bessel transform of $f(s,t)$, known from the data parametrization. Explicitly,

$$2ph(b,s) = i\left[1-e^{i\chi(b)}\right] = 2pf_l(p) + \mathcal{O}\left(s^{-1}\right) = 2\int_0^\infty q\,{\rm d}\,qJ_0(bq)f\left(s,-q^2\right) . \tag{6}$$

In Fig. 1 (b), we demonstrate that the range of the TOTEM data in q is sufficient to carry out this transform to a satisfactory accuracy needed in our analysis.

The standard formulas for the total, elastic, and inelastic cross sections (in our analysis, we treat all the components to the inelastic scattering jointly, not discriminating, *e.g.*, the diffractive components) in the b representation can be parameterized with the eikonal phase $\chi(b)$ and have the form of [28]

$$\sigma_{\rm T} = \frac{4\pi}{p}\,{\rm Im}\, f(s,0) = 4p\int {\rm d}^2b\,{\rm Im}\, h(\vec{b},s) = 2\int {\rm d}^2b\left[1-{\rm Re}\, e^{i\chi(b)}\right] , \tag{7}$$

$$\sigma_{\rm el} = \int {\rm d}\Omega|f(s,t)|^2 = 4p^2\int {\rm d}^2b|h(\vec{b},s)|^2 = \int {\rm d}^2b|1-e^{i\chi(b)}|^2 , \tag{8}$$

$$\sigma_{\rm in} \equiv \sigma_{\rm T}-\sigma_{\rm el} = \int {\rm d}^2b\sigma_{\rm in}(b) = \int {\rm d}^2b\left[1-e^{-2{\rm Im}\chi(b)}\right] , \tag{9}$$

with the integrands $\sigma_{\rm in}(b)$, $\sigma_{\rm el}(b)$ and $\sigma_{\rm T}(b)$ being dimensionless quantities that can be interpreted as the corresponding b-dependent relative number of collisions. For instance, accordingly to Eq. (9), the inelasticity profile is defined as

$$\sigma_{\rm in}(b) = 4p\,{\rm Im}\,h(b,s) - 4p^2|h(b,s)|^2\,. \tag{10}$$

While unitarity implies $\sigma_{\rm in}(b) > 0$, one also has $\sigma_{\rm in}(b) \leq 2k(b,s) - k(b,s)^2$, with $k(b,s) \equiv 2p\,{\rm Im}\,h(b,s)$, and hence one also has the upper bound $\sigma_{\rm in}(b) \leq 1$.

Now, we come to our results. In Fig. 2, we present the real and imaginary parts of the eikonal amplitude $2ph(b)$ for several collision energies. The real parts are smaller from the corresponding imaginary parts, as their ratio is given by the (constant) ρ parameter. The important observation here is that the imaginary parts go above 1 near the origin for the LHC collision energies. We will come back to this issue shortly.

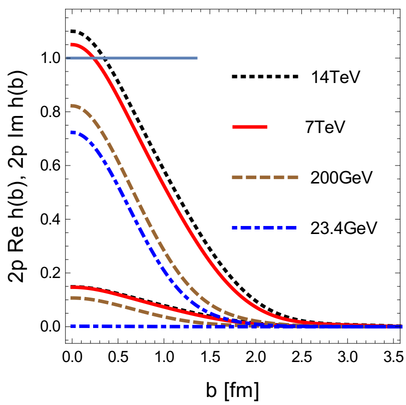

Fig. 2. Real (lower curves) and imaginary (upper curves) parts of the eikonal scattering amplitude $2ph(b)$ for several collision energies. We note that for the LHC energies at the origin, $2p\,{\rm Im}\,h(0) > 1$.

In Fig. 3, we collect the results for the impact-parameter representations of the total, elastic, and inelastic cross sections, as well as for the *edge* function [29, 30], defined as $\sigma_{\rm in}(b) - \sigma_{\rm el}(b)$. The most important feature, visible from Fig. 3 and more accurately form the close-up of Fig. 4, is the *hollowness*: the inelastic cross section develops a minimum at $b = 0$ at the LHC collision energies.

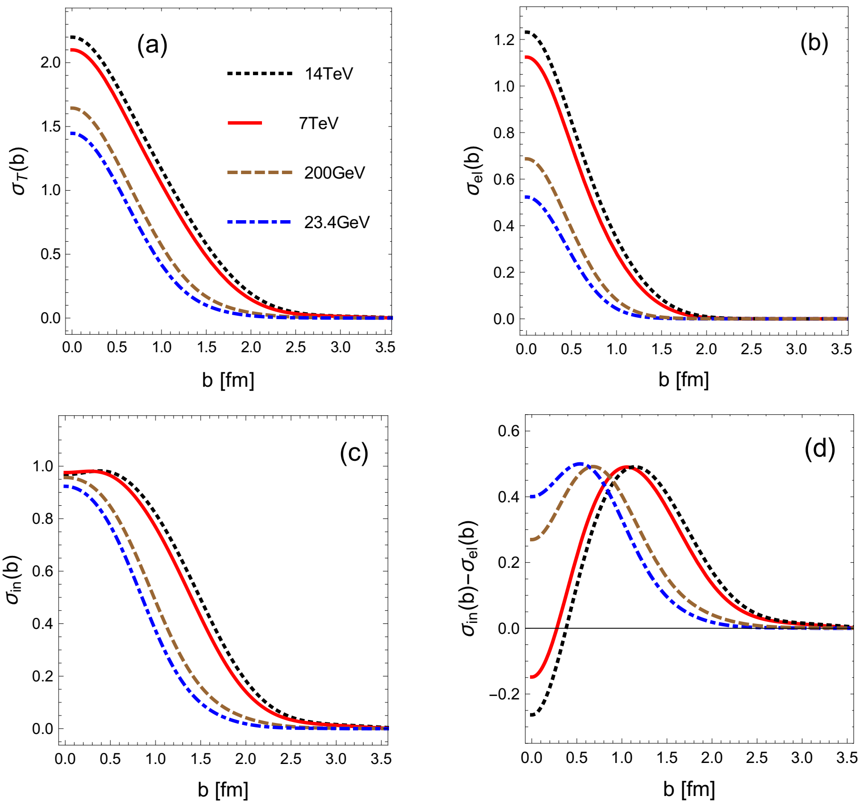

Fig. 3. The total (a), elastic (b), and inelastic (c) cross section, as well as the edge function, plotted as functions of the impact parameter at various collision energies.

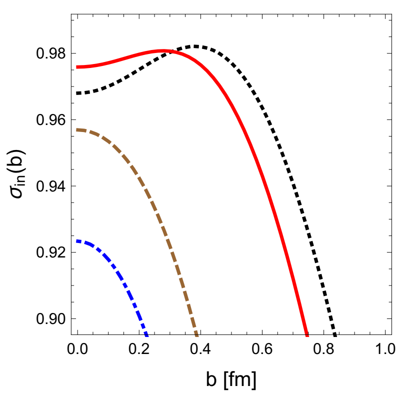

Fig. 4. A close-up of Fig. 3 (c).

To better understand these results, one should resort to the formulas expressed with the eikonal phase, plotted in Fig. 5. We have

$$\begin{aligned} 2p\,\mathrm{Im}\,h(b) &= 1 - e^{-\mathrm{Im}\chi(b)} \cos \mathrm{Re}\chi(b)\,, \\ 2p\,\mathrm{Re}\,h(b) &= e^{-\mathrm{Im}\chi(b)} \sin \mathrm{Re}\chi(b)\,, \\ \sigma_{\mathrm{T}}(b) &= 2 - 2e^{-\mathrm{Im}\chi(b)} \cos \mathrm{Re}\chi(b)\,, \\ \sigma_{\mathrm{el}}(b) &= 1 + e^{-2\mathrm{Im}\chi(b)} - 2e^{-\mathrm{Im}\chi(b)} \cos \mathrm{Re}\chi(b)\,, \\ \sigma_{\mathrm{in}}(b) &= 1 - e^{-2\mathrm{Im}\chi(b)}\,, \\ \sigma_{\mathrm{el}}(b) - \sigma_{\mathrm{in}}(b) &= 2e^{-\mathrm{Im}\chi(b)} \left[\cos \mathrm{Re}\chi(b) - e^{-\mathrm{Im}\chi(b)}\right]\,. \end{aligned} \tag{11}$$

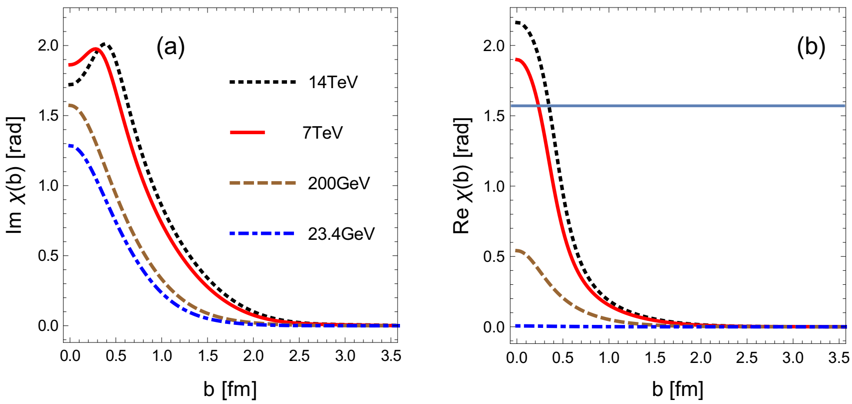

Fig. 5. Imaginary (a) and real (b) part of the eikonal scattering phase, plotted as functions of the impact parameter for several collision energies. We note that at the LHC energies, $\mathrm{Re}\chi(b=0)$ goes above $\pi/2$.

We note several facts following from the above relations:

1. Going of $2p\,\mathrm{Im}\,h(b)$ above 1 and $\sigma_{\mathrm{T}}(b)$ above 2 are caused by $\mathrm{Re}\chi(b) > \pi/2$, where $\cos\mathrm{Re}\chi(b) < 0$ (*cf.* Figs. 2, 3 (a), and 5 (b)).
2. In addition, if $\chi(b) > \pi/2$, the edge function is negative and $\sigma_{\mathrm{el}}(b) > 1$.
3. The departure of $2p\,\mathrm{Im}\,h(b)$ from 1 is of similar order as $2p\,\mathrm{Re}\,h(b)$, with both suppressed with $e^{-\mathrm{Im}\chi(b)}$.

We see that this is the *real* part of the eikonal phase which controls the behavior related to hollowness.

One may give a simple criterion for $\sigma_{\mathrm{in}}(b)$ to develop a minimum at $b=0$. From Eqs. (10) and (3), we get

$$\frac{\mathrm{d}\sigma_{\mathrm{in}}(b)}{\mathrm{d}b^2} = 2p\frac{\mathrm{d}\,\mathrm{Im}\,h(b)}{\mathrm{d}b^2}\left[1 - \left(1+\rho^2\right) 2p\,\mathrm{Im}\,h(b)\right]\,, \tag{12}$$

which is negative at the origin if

$$2p\,\mathrm{Im}\,h(0) > \frac{1}{1+\rho^2} \sim 1\,. \tag{13}$$

Since at the LHC $\rho = 0.14$, the departure of $1/(1+\rho^2)$ from 1 is at the level of 2%.

We also find from Eq. (11) that

$$\frac{\mathrm{d}\sigma_{\mathrm{in}}(b)}{\mathrm{d}b^2} = 2e^{-2\,\mathrm{Im}\chi(b)}\frac{\mathrm{d}\,\mathrm{Im}\chi(b)}{\mathrm{d}b^2}\,, \tag{14}$$

thus the appearance of the dip at the origin in $\sigma_{\mathrm{in}}(b)$ is associated with the dip in $\mathrm{Im}\chi(b)$. This is manifest between Fig. 4 and Fig. 5 (a).

Dremin [8–10] proposed a simple Gaussian model of the amplitude which one may adapt to the presence of the real part of the amplitude (which is crucial for maintaining unitarity with the hollowness effect). One can parametrize the amplitude at low values of b (which is the numerically relevant region) as

$$\mathrm{Im}(2p\,h(p)) = Ae^{-\frac{2b^2}{2B}}\,, \qquad A = \frac{4\sigma_{\mathrm{el}}}{\left(1+\rho^2\right)\sigma_{\mathrm{tot}}}\,, \qquad B = \frac{\left(1+\rho^2\right)\sigma_{\mathrm{tot}}^2}{16\pi\sigma_{\mathrm{el}}}\,. \tag{15}$$

The curvature of the inelasticity profile at the origin is

$$\frac{1}{2}\left.\frac{\mathrm{d}^2 n_{\mathrm{in}}(b)}{\mathrm{d}b^2}\right|_{b=0} = \frac{64\pi\sigma_{\mathrm{el}}^2(4\sigma_{\mathrm{el}}-\sigma_{\mathrm{tot}})}{\left(\rho^2+1\right)^2\sigma_{\mathrm{tot}}^4}\,. \tag{16}$$

We note it changes the sign when $\sigma_{\mathrm{el}} = \frac{1}{4}\sigma_{\mathrm{tot}}$, with the value at the origin

$$\sigma_{\mathrm{in}}(0) = \frac{8\sigma_{\mathrm{el}}}{(1+\rho^2)\sigma_{\mathrm{tot}}}\left(1-2\frac{\sigma_{\mathrm{el}}}{\sigma_{\mathrm{tot}}}\right)\,. \tag{17}$$

As predicted by Dremin, the hollowness effect emerges when $\sigma_{\mathrm{el}} > \frac{1}{4}\sigma_{\mathrm{tot}}$, which is the case of the LHC collision energies. We illustrate relation (17) in Fig. 6.

The final point, very important from the conceptual point of view and for the understanding of the effect, is the impossibility of hollowness to emerge from incoherent folding of inelasticities of collisions of the protons' partonic constituents. In many models incoherent superposition is assumed, *i.e.*, the inelasticity of the pp process is obtained from the folding formula shown below. These ideas have been implemented in microscopic models based on

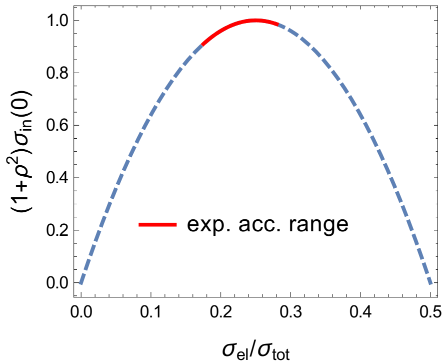

Fig. 6. Illustration of Eq. (17). The solid line corresponds to the experimental values of the ratio of the elastic to total *pp* cross section. Values of $\sigma_{\rm el}/\sigma_{\rm T} > 1/4$ correspond to hollowness in the Gaussian model.

intuitive geometric interpretation [30–35]. Folding involves

$$\begin{aligned}\sigma_{\rm in}(b) \propto & \int {\rm d}^2 b_1 {\rm d}^2 b_2 \rho(\vec{b}_1 + \vec{b}/2) w(\vec{b}_1 - \vec{b}_2) \rho(\vec{b}_2 - \vec{b}/2) \\ = & \int {\rm d}^3 b_1 {\rm d}^3 b_2 \rho(\vec{b}_1) w(\vec{b}_1 - \vec{b}_2) \rho(\vec{b}_2) \\ & -\frac{1}{2} \int {\rm d}^3 b_1 {\rm d}^3 b_2 \left[\vec{b} \cdot \nabla \rho(\vec{b}_1)\right] w(\vec{b}_1 - \vec{b}_2) \left[\vec{b} \cdot \nabla \rho(\vec{b}_2)\right] + \dots\,, \end{aligned} \quad (18)$$

where $w(\vec{b}_1 - \vec{b}_2)$ is a positive-definite kernel (folding models usually take $w(\vec{b}_1 - \vec{b}_2) \propto \delta(\vec{b}_1 - \vec{b}_2)$) and $\rho(\vec{b})$ describes the (possibly correlated) transverse distribution of components in the proton. By passing to the Fourier space, it is simple to show that $\sigma_{\rm in}(b) = \alpha^2 - \beta^2 b^2 + \dots$, with real constants α and β, therefore $\sigma_{\rm in}(b)$ has necessarily a local maximum at $b = 0$, in contrast to the phenomenological hollowness result at the LHC energies. An analogous argument holds for the 3D-hollowness unveiled in our work [1, 2], which takes place already at lower energies.

In conclusion, we stress that the hollowness effect in *pp* scattering at the LHC energies has necessarily a quantum origin. As just shown, it cannot be obtained by an incoherent folding of inelasticities of collisions of partonic constituents. Moreover, we have demonstrated that the real part of the scattering amplitude plays a crucial role in generating hollowness: the effect appears when the real part of the eikonal phase becomes larger than $\pi/2$. *Per se*, there is nothing unusual in that fact. If coherence occurs, the phases of amplitudes from the constituents may add up (as is the case, *e.g.*, in the Glauber model [36]) and at some point, the value of $\pi/2$ may be crossed. A microscopic realization of this quantum mechanism remains, however, a challenge. Finally, we note that in [1, 2], we have presented a three-dimensional interpretation of the effect, which offers an even more pronounced hollowness feature.

REFERENCES

[1] E. Ruiz Arriola, W. Broniowski, *Few Body Syst.* **57**, 485 (2016) [arXiv:1602.00288 [hep-ph]]
[2] E. Ruiz Arriola, W. Broniowski, *Phys. Rev. D* **95**, 074030 (2017) [arXiv:1609.05597 [nucl-th]].
[3] G. Antchev *et al.* [TOTEM Collaboration], *Europhys. Lett.* **101**, 21002 (2013).
[4] G. Aad *et al.* [ATLAS Collaboration], *Nucl. Phys. B* **889**, 486 (2014) [arXiv:1408.5778 [hep-ex]].
[5] G. Antchev *et al.* [TOTEM Collaboration], *Phys. Rev. Lett.* **111**, 012001 (2013).
[6] M. Aaboud *et al.* [ATLAS Collaboration], *Phys. Lett. B* **761**, 158 (2016) [arXiv:1607.06605 [hep-ex]].
[7] A. Alkin, E. Martynov, O. Kovalenko, S.M. Troshin, *Phys. Rev. D* **89**, 091501 (2014) [arXiv:1403.8036 [hep-ph]].
[8] I.M. Dremin, *Bull. Lebedev Phys. Inst.* **42**, 21 (2015) [*Kratk. Soobshch. Fiz.* **42**, 8 (2015)] [arXiv:1404.4142 [hep-ph]].
[9] I.M. Dremin, *Phys. Usp.* **58**, 61 (2015) [arXiv:1406.2153 [hep-ph]].
[10] I.M. Dremin, arXiv:1610.07937 [hep-ph].
[11] I.M. Dremin, arXiv:1702.06304 [hep-ph].
[12] V.V. Anisovich, V.A. Nikonov, J. Nyiri, *Phys. Rev. D* **90**, 074005 (2014) [arXiv:1408.0692 [hep-ph]].
[13] S.M. Troshin, N.E. Tyurin, *Mod. Phys. Lett. A* **31**, 1650079 (2016) [arXiv:1602.08972 [hep-ph]].
[14] S.M. Troshin, N.E. Tyurin, *Eur. Phys. J. A* **53**, 57 (2017) [arXiv:1701.01815 [hep-ph]].
[15] S.M. Troshin, N.E. Tyurin, arXiv:1704.00443 [hep-ph].
[16] J.L. Albacete, A. Soto-Ontoso, *Phys. Lett. B* **770**, 149 (2017) [arXiv:1605.09176 [hep-ph]].
[17] D.A. Fagundes *et al.*, *Phys. Rev. D* **88**, 094019 (2013) [arXiv:1306.0452 [hep-ph]].
[18] R.J.N. Phillips, V.D. Barger, *Phys. Lett. B* **46**, 412 (1973).
[19] U. Amaldi, K.R. Schubert, *Nucl. Phys. B* **166**, 301 (1980).
[20] G. Antchev *et al.* [TOTEM Collaboration], *Eur. Phys. J. C* **76**, 661 (2016) [arXiv:1610.00603 [nucl-ex]].

[21] J.L. Bailly *et al.* [EHS-RCBC Collaboration], *Z. Phys. C* **37**, 7 (1987).

[22] G.B. West, D.R. Yennie, *Phys. Rev.* **172**, 1413 (1968).

[23] R. Cahn, *Z. Phys. C* **15**, 253 (1982).

[24] M.M. Block, R.N. Cahn, *Rev. Mod. Phys.* **57**, 563 (1985).

[25] J. Prochazka, V. Kundrat, `arXiv:1606.09479 [hep-th]`.

[26] G. Aielli *et al.* [ARGO-YBJ Collaboration], *Phys. Rev. D* **80**, 092004 (2009) [`arXiv:0904.4198 [hep-ex]`].

[27] S.L. Bueltmann *et al.*, *Phys. Lett. B* **579**, 245 (2004) [`arXiv:nucl-ex/0305012`].

[28] R. Blankenbecler, M.L. Goldberger, *Phys. Rev.* **126**, 766 (1962).

[29] M.M. Block *et al.*, *Phys. Rev. D* **91**, 011501 (2015) [`arXiv:1409.3196 [hep-ph]`].

[30] M.M. Block, L. Durand, P. Ha, F. Halzen, *Phys. Rev. D* **92**, 014030 (2015) [`arXiv:1505.04842 [hep-ph]`].

[31] T.T. Chou, C.-N. Yang, *Phys. Rev.* **170**, 1591 (1968).

[32] T.T. Chou, C.-N. Yang, *Phys. Rev.* **175**, 1832 (1968).

[33] H. Cheng, T.T. Wu, *Expanding Protons: Scattering at High Energies*, Mit Press, 1987.

[34] C. Bourrely, J. Soffer, T.T. Wu, *Phys. Rev. D* **19**, 3249 (1979).

[35] M.M. Block, *Phys. Rep.* **436**, 71 (2006) [`arXiv:hep-ph/0606215`].

[36] R. Glauber, *High Energy Collision Theory, Vol. 1*, in: Lectures in Theoretical Physics, Interscience, New York 1959.